

Exploring phase diagram of $N_f = 3$ QCD at $\mu = 0$ with HISQ fermions

H.-T. Ding*, A. Bazavov, P. Hegde, F. Karsch, S. Mukherjee and P. Petreczky

Physics Department, Brookhaven National Laboratory, Upton, NY 11973

E-mail: htding@quark.phy.bnl.gov

We studied the QCD phase transition as a function of quark mass in the $N_f = 3$ QCD at vanishing baryon density. Lattice simulations have been performed using Highly Improved Staggered Quarks on $N_\tau = 6$ lattices with quark masses that correspond to pion masses in the region $80 \lesssim m_\pi \lesssim 230$ MeV. We found no evidence of the first order phase transition in the current pion mass window. The pion mass at the critical point where the first order phase transition starts is estimated to be $m_\pi^c \lesssim 45$ MeV.

XXIX International Symposium on Lattice Field Theory

July 10-16 2011

Squaw Valley, Lake Tahoe, California

*Speaker.

1. Introduction

It has been well established that at a certain high temperature and large baryon density the hadronic matter will undergo a phase transition [1, 2]. The nature of the phase transition depends on the quark mass and its number of flavors. As shown in the left plot of Fig. 1 at vanishing baryon density, in upper right corner, i.e. pure gauge case with infinitely heavy quark mass, there exists a first order phase transition, where the Polyakov loop may serve as an order parameter. With decreasing quark mass, the first order transition will be weakened and is separated from the cross over region by a second order phase transition line. In the chiral limit, i.e. in the lower left corner of the left plot in Fig. 1, for 3 flavors, there exists a first order phase transition, whose order parameter is the chiral condensate. This first order chiral phase transition extends to a certain region with finite quark mass and ends at a second order phase transition line, which separates the cross over region from the first order phase transition region. The universal properties of this line of the second transition are expected to be controlled by a global $Z(2)$ symmetry, which however is not an obvious global symmetry of the QCD Lagrangian. It is obvious that neither the chiral condensate or the Polyakov loop is an adequate order parameter for the spontaneous $Z(2)$ symmetry breaking, and instead the true order parameter is obtained by mixing the chiral condensate with the energy density [3]. When the chemical potential is turned on, the second order boundary lines turn into surfaces, as shown in the right plot of Fig. 1. The qualitative features of the $(T - \mu)$ phase diagram depends on the curvature of the surface at $\mu = 0$. The common expectation is that this curvature is positive and there exists a chiral critical point at μ_c . This expectation seems to be confirmed by lattice simulation using improved p4 action [4]. Calculations using standard staggered action on $N_\tau = 4$ lattices on the other hand indicate a negative curvature [5]. Thus this issue needs to be resolved in the future.

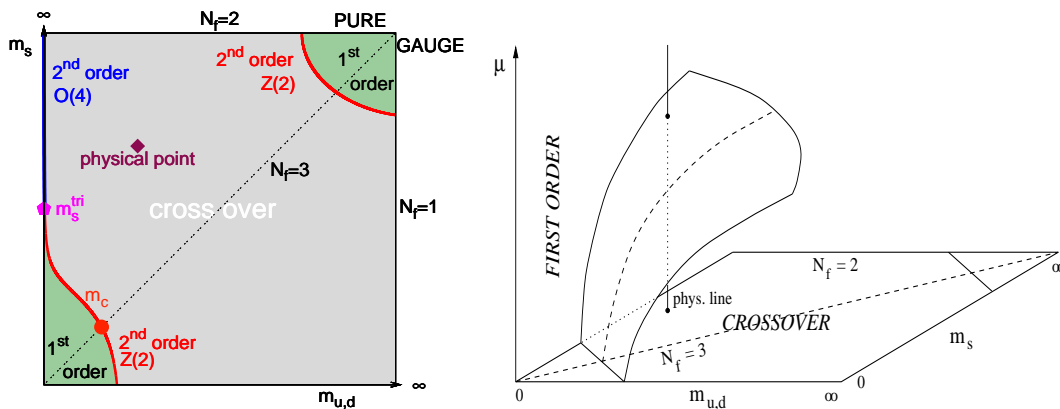


Figure 1: Left: schematic QCD phase transition behavior for different choices of quark masses ($m_{u,d}, m_s$) at zero chemical potential. Right: The critical surface swept by the chiral critical line at finite chemical potential. A QCD chiral critical point may exist if the surface bends towards to the physical point. The right plot is taken from Ref. [4].

To what extent the first order phase transition holds at $\mu = 0$ is of our current primary interests. Previous estimations using linear sigma model gives the pion mass at the critical point to be around 50 MeV [4, 6] and most recent calculations with complete one-loop parametrization of the linear

sigma model predict critical pion mass to be around 110 MeV [7]. Here through lattice QCD simulations we focus on the case with three degenerate quark masses, which corresponds to the dotted diagonal line shown in the left plot of Fig. 1, i.e. to determine the chiral critical point in the 3-flavor QCD. The boundary of the chiral first order phase transition in the 3-flavor QCD has been investigated using standard staggered actions [5, 8–10] as well as improved staggered actions (p4, asqtad and stout) [3, 4, 11–14]. There is a significant discrepancy of the quark masses, or the equivalently the pion masses at the chiral critical point from the above studies. Using the standard staggered action it was found that the pion mass at the critical point is about 300 MeV [8, 9], while using improved p4 action the critical pion mass is about 70 MeV [4]. The above results are obtained on the lattices with the temporal extent $N_\tau = 4$. Other calculations using p4 and asqtad actions on finer lattices disfavor critical pion mass of 300 MeV [12, 13]. With large N_τ , i.e. $N_\tau = 6$, it has been shown that the pion mass on the critical lines becomes smaller compared with the one with $N_\tau = 4$ using standard staggered fermions [5]. Investigations on $N_\tau = 6$ lattices have also been performed using improved (stout) action, in which three quark flavors are not degenerate and the ratio of light to strange quark is fixed to be about 1/27 when approaching the massless limit [14]. The analysis in Ref. [14] suggests that the critical pion mass is about 50 MeV. Thus the first order phase transition becomes weaker when approaching the continuum limit ¹.

2. Lattice parameters

As mentioned before, the first order phase transition region from lattice QCD simulations shrinks with reduced cut-off effects. The Highly Improved Staggered Quark (HISQ) action, which is developed by the HPQCD/UKQCD collaboration [16], achieves better taste symmetry than the asqtad and p4 actions at a given lattice spacing. The improvements in HISQ action designed to reduce taste symmetry violations can translate into smaller lattice spacing dependences in other quantities and it has been found that the net results from HISQ simulations at lattice spacing a appear to have similar lattice artifacts as that from asqtad simulations at lattice spacing $\frac{2}{3}a$ [17]. Thus the HISQ simulations, which will be used in our simulations, can save substantial computing costs and can be essentially useful to get better understanding of the chiral first order phase transition region. Simulations have been carried out with 3 degenerate quark flavors. The quark masses vary from 0.0075 to 0.0009375 corresponding to pion masses in the region of $80 \lesssim m_\pi \lesssim 230$ MeV. The parameters of our simulations are given in Table 1.

3. Universality class near critical lines

In the vicinity of the critical lines, the free energy may be expressed as a sum of a regular and a singular part,

$$f = \frac{-T}{V} \ln Z \equiv f_{\text{sing}}(t, h) + f_{\text{reg}}(T, m). \quad (3.1)$$

¹The first order phase transition also becomes weaker in the continuum limit from the study of 4-flavor QCD using HYP action [15].

lattice dim.	am_q	m_π [MeV]	# β values	max. no. of traj.
$16^3 \times 6$	0.0075	230	17	6000
$24^3 \times 6$	0.00375	160	12	7900
$24^3 \times 6$	0.001875	110	7	8800
$24^3 \times 6$	0.00125	90	7	5100
$24^3 \times 6$	0.0009375	80	8	6300
$16^3 \times 6$	0.0009375	80	6	7100

Table 1: Parameters of the numerical simulations.

The singular part of the free energy $f_{\text{sing}}(t, h)$ is most relevant to the QCD phase transitions and dominates when system is close to the critical lines. The order parameter M of the transition is controlled by a scaling function that arises from the singular part of the free energy [18, 19]

$$M(t, h) = -\partial f_{\text{sing}}(t, h)/\partial h = f_G(z), \quad (3.2)$$

where $f_G(z)$ is the universal scaling function and $z = t/h^{1/\beta\delta}$. β and δ are universal critical exponents. Here scaling variables t and h measure how far the system is away from the criticality. They are related to the temperature T and the symmetry breaking (magnetic) field H ,

$$t = \frac{1}{t_0} \frac{T - T_c}{T_c}, \quad h = \frac{H}{h_0} = \frac{1}{h_0} \frac{m - m_c}{m_c}, \quad (3.3)$$

where T_c is the transition temperature when external field H vanishes, i.e. $m = m_c$. m_c is the critical quark mass where transition occurs. t_0 and h_0 are normalization factors.

In the two flavor QCD, the order parameter M for the chiral transition is the chiral condensate and the critical mass m_c is zero, thus the chiral condensate and chiral susceptibility have the following relations

$$M = \langle \bar{\psi}\psi \rangle / T^3 \Big|_{\text{fixed } z} \propto m^{1/\delta}, \quad \chi_q / T^2 \Big|_{\text{fixed } z} \propto m^{1/\delta-1}. \quad (3.4)$$

In the three flavor QCD, as mentioned before, there is a first order phase transition in the chiral limit, which extends to a critical quark mass m_c and ends at a second order phase transition line. It is expected that the universal properties of this critical point are controlled by a global $Z(2)$ symmetry. The proper order parameter should be a mixing of two transition relevant quantities, e.g. a combination of the chiral condensate with the pure gauge action S_G [3]

$$M = (\langle \bar{\psi}\psi \rangle + rS_G) \Big|_{T=T_c, m_c} \propto (m - m_c)^{1/\delta} \quad (3.5)$$

and the susceptibility of the order parameter M

$$\chi_M / T^2 \Big|_{T=T_c, m_c} \propto (m - m_c)^{1/\delta-1}. \quad (3.6)$$

Here $1/\delta - 1$ for $Z(2)$ universal class is -0.785. With standard staggered action, it is important to construct the correct order parameter since $\langle \bar{\psi}\psi \rangle$ is large [10]. With improved fermion action, e.g. HISQ, one may consider the effect from the mixing of the energy field is small since $\langle \bar{\psi}\psi \rangle$ is closer to zero. To make estimates on the value of m_c , we will use the quark chiral condensate as an approximate order parameter for the second order phase transition at the critical point.

4. Results

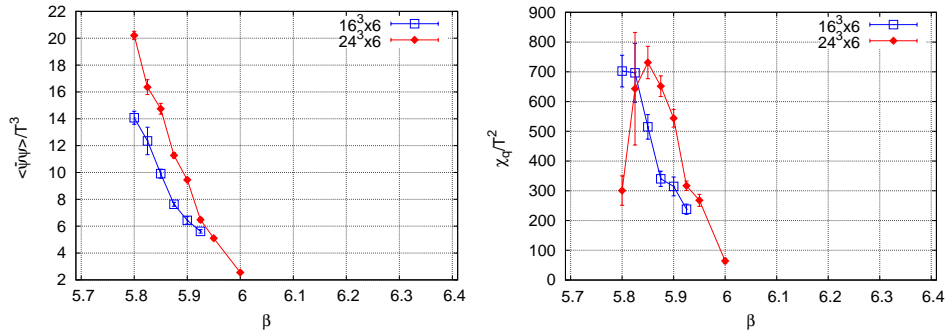


Figure 2: Volume dependences of the chiral condensate (left) and the chiral susceptibility (right) with quark mass $am = 0.0009375$.

We first look at the volume dependence of quark chiral condensate at $am = 0.0009375$ ($m_\pi \approx 80$ MeV) shown in the left plot of Fig. 2. The volume dependence at high temperature is small while at low temperature is relatively large. This is obvious since at high temperature the scale of the system is controlled by the temperature T while at low temperature the scales are the hadron masses. In the right plot of Fig. 2 we show the volume dependences of the chiral susceptibility. If the system with quark mass $am = 0.0009375$ is in the first order phase transition region, the chiral susceptibility should scale with the volume. However, such volume scaling behavior is not observed with pion mass $m_\pi \approx 80$ MeV.

In the left plot of Fig. 3, we show the time history of quark chiral condensate near pseudo critical beta value with our lowest quark mass on $24^3 \times 6$ lattices. There is no evidence for the coexistence of two phases. We then investigate the temperature dependence of the chiral condensate at different quark masses shown in the right plot Fig. 3. No evidence of the discontinuity of $\langle \bar{\psi}\psi \rangle$ in β at all quark masses is found. Together with the evidence from Fig. 2 we conclude that there is no first order phase transition even with quark mass down to 0.0009375 ($m_\pi \approx 80$ MeV).

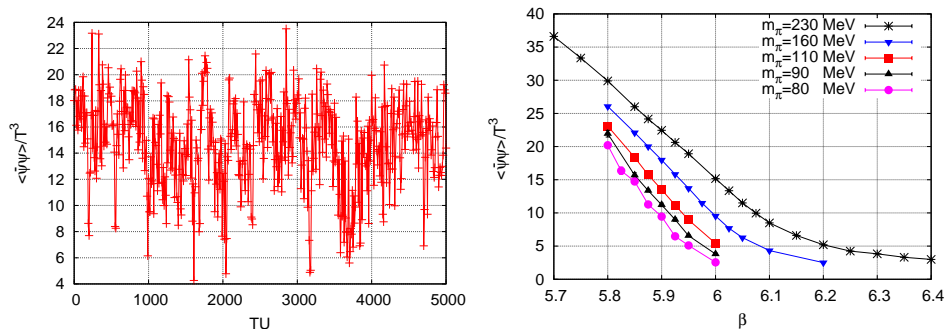


Figure 3: Left: time history of the quark chiral condensate near β_c with $am = 0.0009375$ on $24^3 \times 6$ lattices. Right: chiral condensates as a function of β .

In the left plot of Fig. 4 we show the disconnected part of the chiral susceptibility as a function of quark mass. The pseudo critical temperature becomes smaller with smaller quark mass. This can

be explained as that the hadronic degrees of freedom in the system become lighter and thus they become more easily excited in the thermal heat bath. They then can contribute to the energy density of the system and thus trigger the onset of a phase transition already at a lower temperature. The peak height of chiral susceptibility grows with decreasing quark mass as the system is approaching the first order phase transition region. We then performed a scaling fit according to Eq. (3.6) to the chiral susceptibility peaks. The results are shown in the right plot of Fig. 4. As the finite volume effects would bring the peak height of chiral susceptibility up, we can get a upper bound for this analysis, which gives the pion mass at the critical point $m_\pi^c \lesssim 45$ MeV.

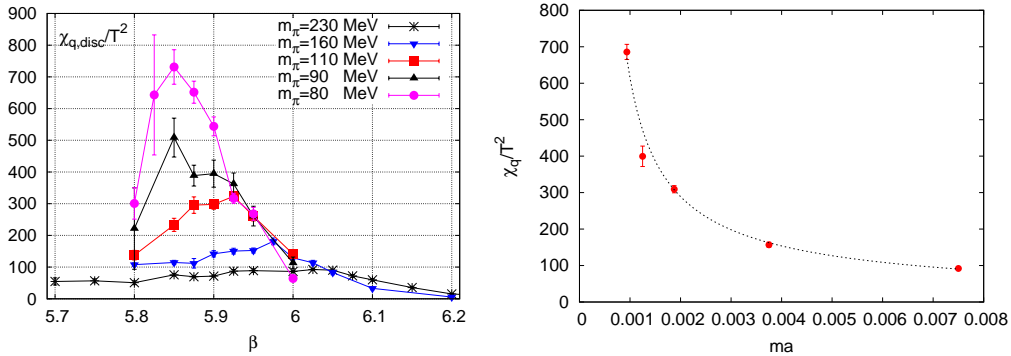


Figure 4: Left: the disconnected part of the chiral susceptibility as a function of β . Right: the scaling fit to the height of chiral susceptibility peaks.

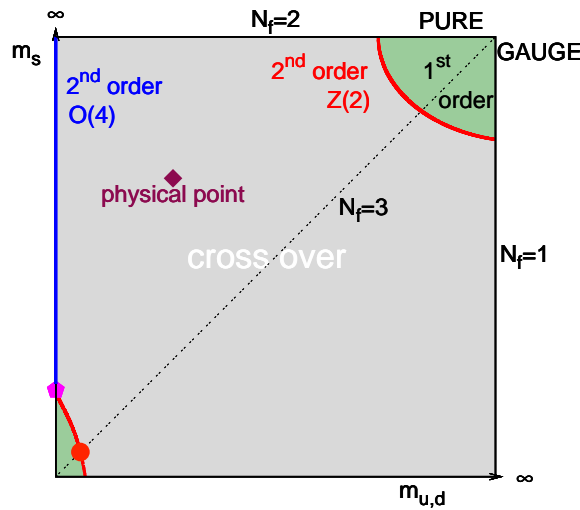


Figure 5: QCD phase diagram at vanishing baryon density in the quark mass plane.

5. Conclusion

We have performed 3-flavor QCD simulations using HISQ/tree action on $N_\tau = 6$ lattices with five pion masses in the region of $80 \lesssim m_\pi \lesssim 230$ MeV. Through the study of quark chiral condensates and chiral susceptibilities, we found no evidence of the first order chiral phase transition

in this pion mass region. The upper bound of the pion mass at the critical point is estimated to be around 45 MeV. It means that in the quark mass plane, the coordinate of the furthest critical point from the origin in the 3-flavor QCD is at about $(m_{\text{phy}}^s/270, m_{\text{phy}}^s/270)$, which is very far away from the physical point at $(m_{\text{phy}}^s/27, m_{\text{phy}}^s)$, as sketched in Fig. 5. Together with the results from Ref. [14], our results suggest that the first order phase transition region is very small and thus the critical surface swept by the chiral critical line at finite chemical potential has to be bent towards to the physical point with a very large curvature to affect the nature of the real world at a small chemical potential.

6. Acknowledgements

The numerical simulations were carried out on clusters of the USQCD Collaboration in Jefferson Lab and Fermilab, and on BlueGene/L computers at the New York Center for Computational Sciences (NYCCS) at Brookhaven National Lab. This manuscript has been authored under contract number DE-AC02-98CH10886 with the U.S. Department of Energy.

References

- [1] F. Karsch, Lect. Notes Phys. **583**, 209 (2002).
- [2] K. Fukushima, T. Hatsuda, Rept. Prog. Phys. **74**, 014001 (2011). [arXiv:1005.4814 [hep-ph]].
- [3] F. Karsch, E. Laermann and C. Schmidt, Phys. Lett. B **520**, 41 (2001).
- [4] F. Karsch, C. R. Allton, S. Ejiri, S. J. Hands, O. Kaczmarek, E. Laermann, C. Schmidt, Nucl. Phys. Proc. Suppl. **129**, 614-616 (2004). [hep-lat/0309116].
- [5] P. de Forcrand, S. Kim and O. Philipsen, PoS **LAT2007**, 178 (2007) [arXiv:0711.0262 [hep-lat]].
- [6] T. Herpay, A. Patkos, Z. Szep, P. Szepfalusy, Phys. Rev. **D71**, 125017 (2005). [hep-ph/0504167].
- [7] T. Herpay and Z. Szep, Phys. Rev. D **74**, 025008 (2006) [arXiv:hep-ph/0604086].
- [8] N.H. Christ and X. Liao, Nucl. Phys. B (Proc. Suppl.) **119**, 514 (2003).
- [9] P. de Forcrand and O. Philipsen, Nucl. Phys. Proc. Suppl. **129**, 521 (2004).
- [10] D. Smith, C. Schmidt, [arXiv:1109.6729 [hep-lat]].
- [11] C. Schmidt, *et al.*, Nucl. Phys. Proc. Suppl. **119**, 517 (2003) [arXiv:hep-lat/0209009].
- [12] C. Bernard *et al.* [MILC Collaboration], Phys. Rev. **D71**, 034504 (2005). [hep-lat/0405029].
- [13] M. Cheng *et al.*, Phys. Rev. D **75**, 034506 (2007).
- [14] G. Endrodi, Z. Fodor, S. D. Katz, K. K. Szabo, PoS **LAT2007**, 182 (2007). [arXiv:0710.0998].
- [15] A. Hasenfratz and F. Knechtli, arXiv:hep-lat/0105022.
- [16] E. Follana *et al.* [HPQCD and UKQCD Collaborations], Phys. Rev. **D75**, 054502 (2007).
- [17] A. Bazavov *et al.* [MILC collaboration], Phys. Rev. D **82**, 074501 (2010).
- [18] S. Ejiri *et al.*, Phys. Rev. D **80**, 094505 (2009) [arXiv:0909.5122 [hep-lat]].
- [19] F. Karsch, [arXiv:1007.2393 [hep-lat]].